Supporting Information

Hierarchical Multi-Component Nanofiber Separators for Lithium Polysulfide Capture in Lithium-Sulfur Batteries: An Experimental and Molecular Modeling Study

Jiadeng Zhu,[a] Erol Yildirim,[a] Karim Aly,[a] Jialong Shen,[a] Chen Chen,[a] Yao Lu,[a] Mengjin Jiang,[a] David Kim,[b] Alan E. Tonelli,[a] Melissa A. Pasquinelli,[a] Philip D. Bradford,[a] and Xiangwu Zhang*[a]

[a] Fiber and Polymer Science Program, Department of Textile Engineering, Chemistry and Science, North Carolina State University, Raleigh, NC 27695-8301, USA

[b] Sceye, Inc., 1020 19th St NW, Washington, DC 20036, USA

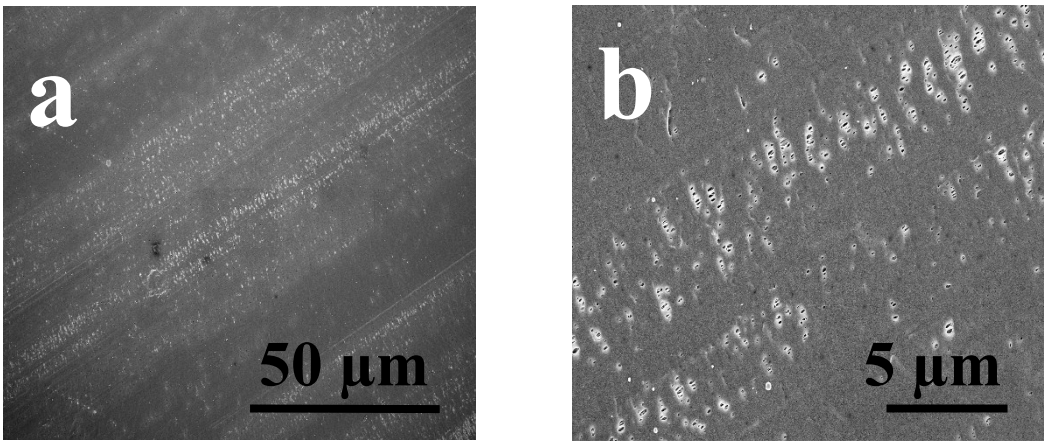

Fig. S1 SEM images of microporous polypropylene separator.

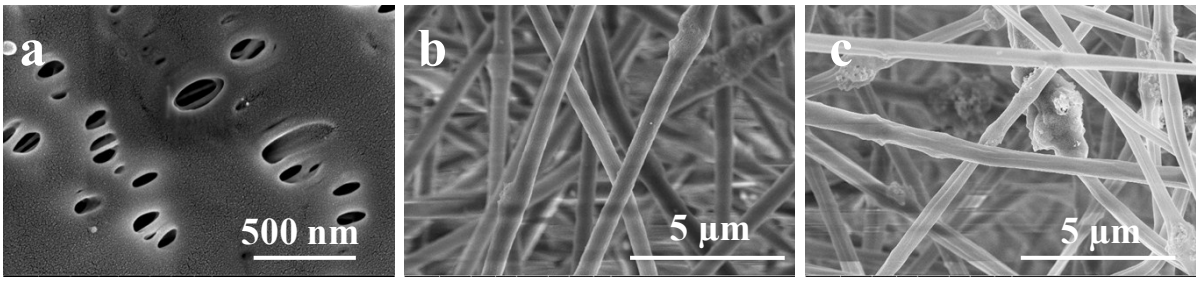

Fig. S2 High maganification SEM images of a) PP, b) PAN/SiO_2-10, and c) PAN/SiO_2-30.

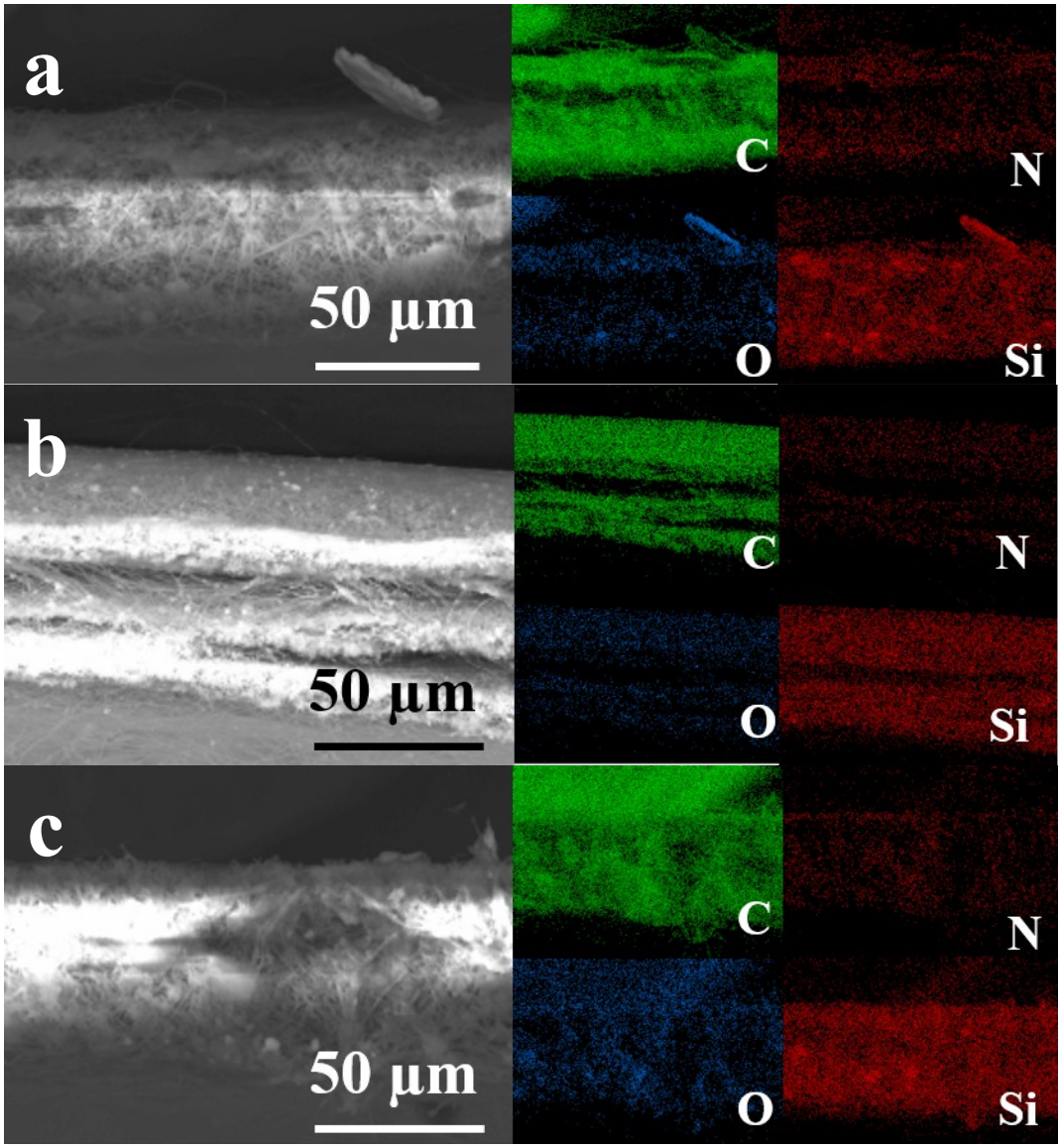

Fig. S3 Cross-sectional SEM images of PAN/SiO_2-10, PAN/SiO_2-30, and PAN/SiO_2-30-MWCNT with the energy-dispersive X-ray (EDX) elemental mappings.

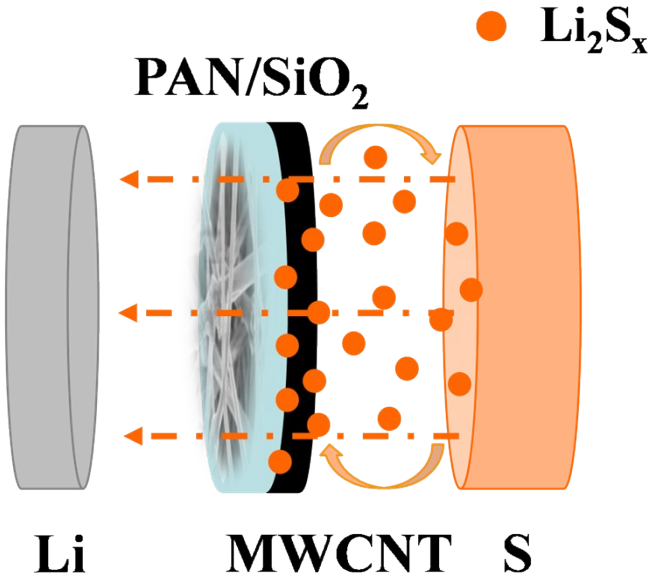

Fig. S4 Schematic illustration of polysulfide diffusion in the Li-S cell with PAN/SiO_2-30-MWCNT.

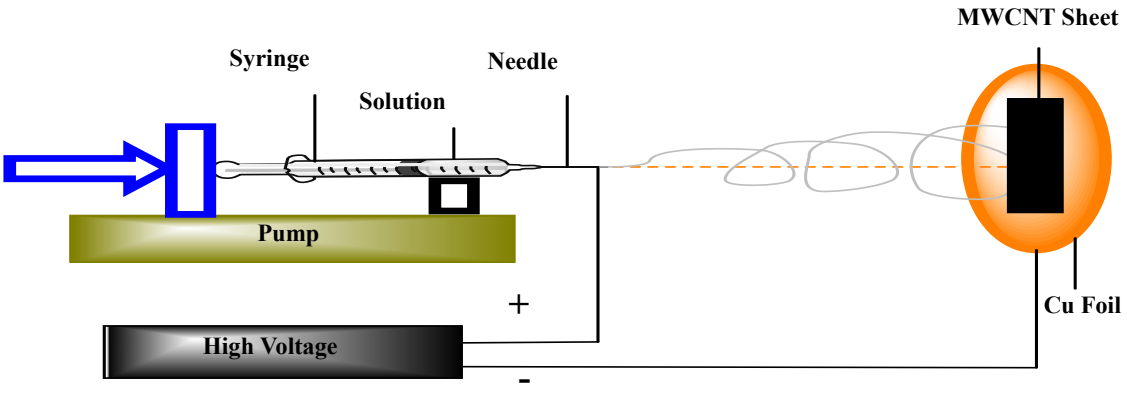

Fig. S5 Schematic image of preparing PAN/SiO_2-30 with MWCNT sheet.

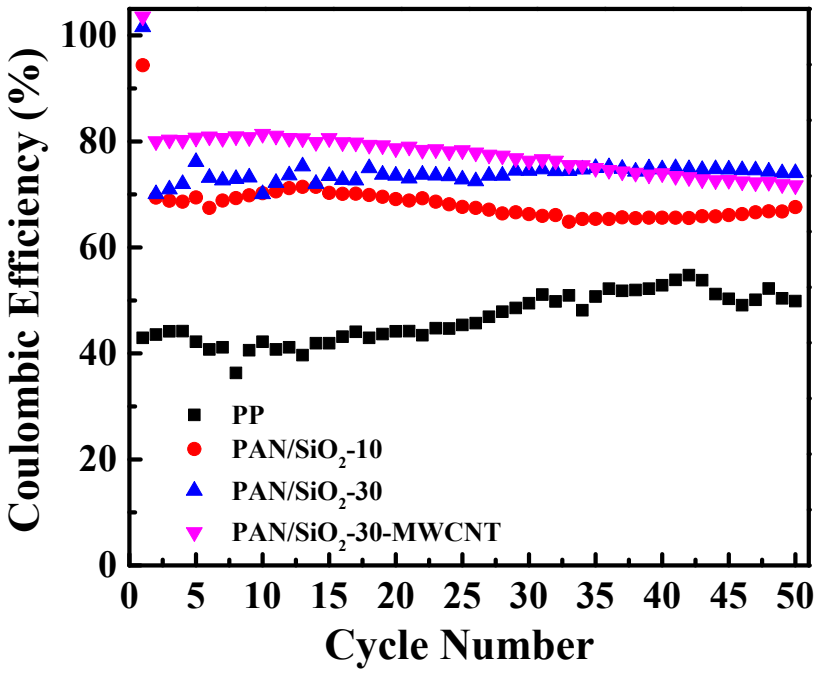

Fig. S6 Coulombic efficiency of Li-S cells by using $LiNO_3$-free electrolyte at a current density of 0.2C.

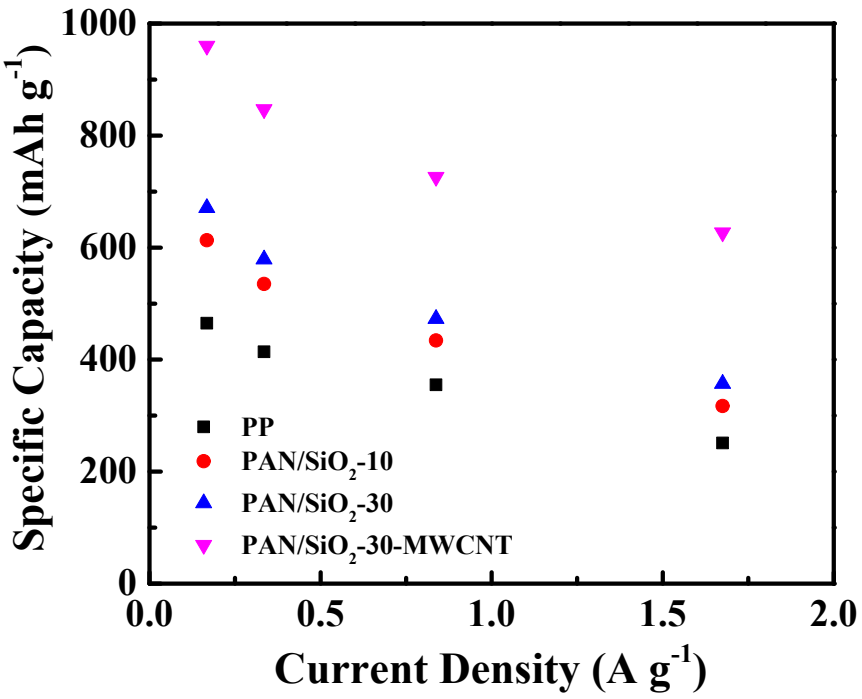

Fig. S7 Comparison of rate capabilities of the Li-S cells with differnt separators.

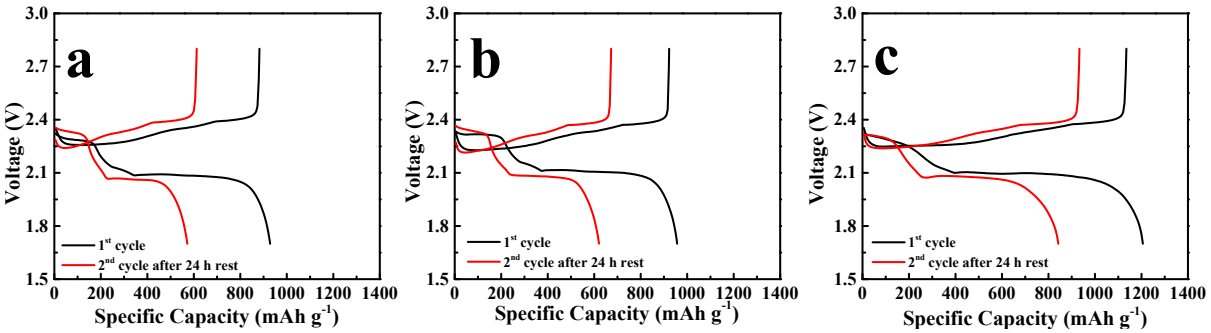

Fig. S8 Self-discharge measurement for the cells with a) PAN/SiO_2-10, b) PAN/SiO_2-30, and PAN/SiO_2-30-MWCNT.

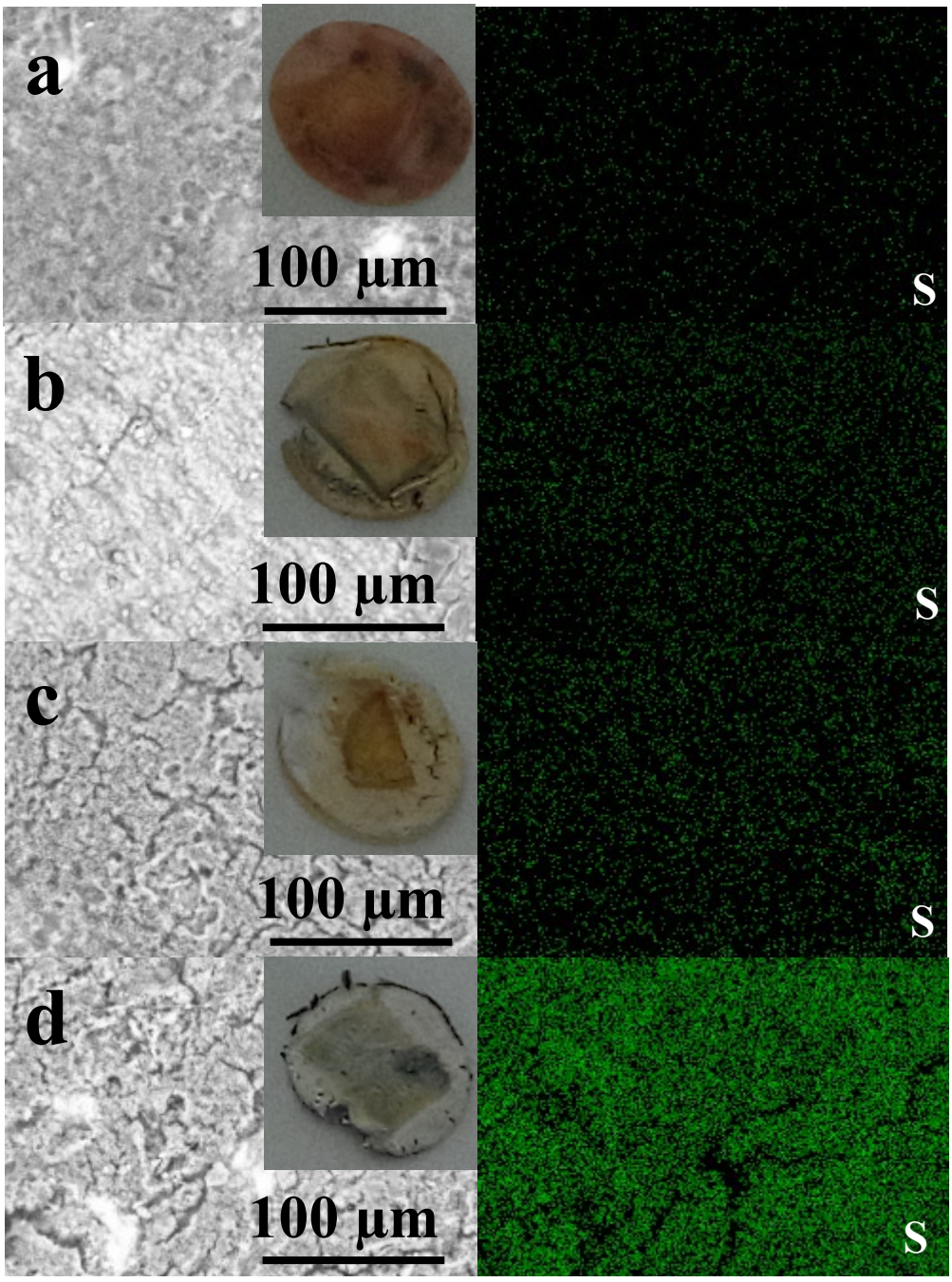

Fig. S9 SEM images and the corresponding S element mapping images of the cathodes after 50 cycles at a current density of 1C: a) PP, b) PAN/SiO_2-10, c) PAN/SiO_2-30, and d) PAN/SiO_2-30-MWCNT separators. The insets are the digital photographs of the separators on the lithium metal side.

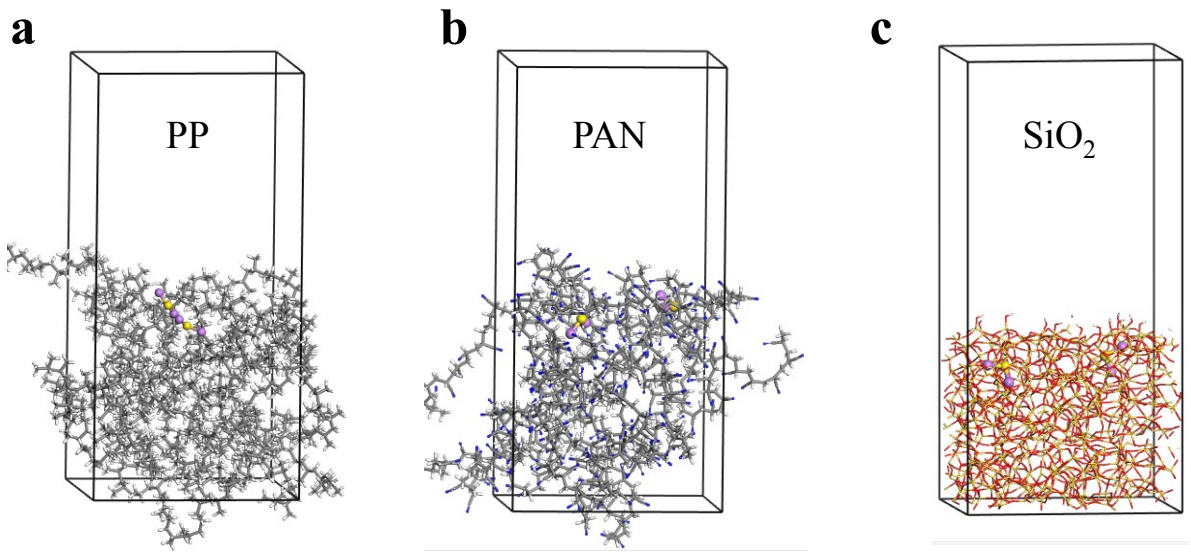

Fig. S10 Stable structures for a) PP, b) PAN and c) SiO_2 surfaces adsorbing two Li_2S molecules (shown in purple/yellow).

Table S1 Elemental composition measurement for PAN/SiO_2-10, PAN/SiO_2-30, and PAN/SiO_2-30-MWCNT membranes.

Material	**Electment (wt%)**			
	C	N	Si	O
PAN/SiO_2-10	69.5	17.6	2.8	10.0
PAN/SiO_2-30	69.9	9.3	4.5	16.2
PAN/SiO_2-30-MWCNT	80.1	6.2	3.4	10.3

Table S2 Binding energy of PP, PAN, SiO_2 with Li_2S and LiS· radical calculated with DFT using both the BLY3P and M06-2X functionals.

Material	Binding Energy (kcal mol^{-1})			
	Li_2S		LiS·	
	B3LYP	M06-2X	B3LYP	M06-2X
PP	-5.99	-6.38	-7.70	-9.23
PAN	-39.57	-49.75	PAN1: -20.82 PAN2: -32.33	PAN1:- 26.81 PAN2: -41.18
SiO_2	-59.75	-76.32	-37.51	-51.91

Table S3 Adsorption energy, rigid adsorption energy and relaxation energy of Li_2S with PP, PAN, and SiO_2 surfaces calculated with Monte Carlo simulations.

Surface	# Adsorbant Li_2S	Adsoption Energy (kcal mol^{-1})	Rigid Adsorption Energy (kcal mol^{-1})	Relaxation Energy (kcal mol^{-1})
PP	**1**	-53.23	-11.36	-41.85
	2	-138.30	-59.47	-81.89
	3	-236.28	-123.57	-112.02
	4	-326.27	-179.52	-146.25
	5	-427.94	-240.48	-187.46
	6	-533.27	-306.54	-225.67
	7	-627.42	-365.72	-257.68
PAN	**1**	-92.08	-52.72	-40.45
	2	-179.17	-104.88	-74.78
	3	-271.54	-151.31	-120.18
	4	-359.90	-209.01	-151.89
	5	-455.26	-260.17	-195.09
	6	-552.11	-316.34	-225.51
	7	-653.12	-373.45	-269.76
SiO_2	**1**	-204.21	-18.18	-186.22
	2	-407.82	-35.41	-372.92
	3	-610.32	-52.62	-557.98
	4	-803.68	-62.85	-744.42
	5	-1008.83	-78.87	-930.96
	6	-1203.66	-87.94	-1115.94
	7	-1396.22	-95.32	-1303.87

Table S4 Li-ion diffusion coefficient measurement.

Sample	Li-ion diffusion coefficient ($cm^2\ s^{-1}$)		
	A	B	C
PAN/SiO_2-10	6.17×10^{-9}	9.56×10^{-9}	2.33×10^{-8}
PAN/SiO_2-30	1.05×10^{-8}	2.05×10^{-8}	3.66×10^{-8}
PAN/SiO_2-30-MWCNT	1.12×10^{-8}	2.09×10^{-8}	4.55×10^{-8}
PP (Ref. 27)	2.90×10^{-9}	6.36×10^{-9}	1.07×10^{-8}
PAN (Ref. 27)	5.51×10^{-9}	6.71×10^{-9}	1.55×10^{-8}